Experimental Laboratory Research

Resting-State Functional Magnetic Resonance Imaging: The Impact of Regression Analysis

Chia-Jung Yeh, MS, Yu-Sheng Tseng, MS, Yi-Ru Lin, PhD, Shang-Yueh Tsai, PhD, Teng-Yi Huang, PhD

From the Department of Electrical Engineering, National Taiwan University of Science and Technology, Taipei, Taiwan, R.O.C (CJY, YST, TYH); Department of Electronic Engineering, National Taiwan University of Science and Technology, Taipei, Taiwan, R.O.C (YRL); and Graduate Institute of Applied Physics, National Chengchi University, Taipei, Taiwan, R.O.C (SYT).

ABSTRACT

PURPOSE

To investigate the impact of regression methods on resting-state functional magnetic resonance imaging (rsfMRI). During rsfMRI preprocessing, regression analysis is considered effective for reducing the interference of physiological noise on the signal time course. However, it is unclear whether the regression method benefits rsfMRI analysis.

MATERIALS AND METHODS

Twenty volunteers (10 men and 10 women; aged 23.4 ± 1.5 years) participated in the experiments. We used node analysis and functional connectivity mapping to assess the brain default mode network by using five combinations of regression methods.

RESULTS

The results show that regressing the global mean plays a major role in the preprocessing steps. When a global regression method is applied, the values of functional connectivity are significantly lower ($P \leq .01$) than those calculated without a global regression. This step increases inter-subject variation and produces anticorrelated brain areas.

CONCLUSION

rsfMRI data processed using regression should be interpreted carefully. The significance of the anticorrelated brain areas produced by global signal removal is unclear.

Keywords: rsfMRI, resting state, default mode network, functional connectivity, regression.

Acceptance: Received June 12, 2013, and in revised form August 28, 2013. Accepted for publication September 29, 2013.

Correspondence: Address correspondence to Teng-Yi Huang, PhD. E-mail: tyhuang@mail.ntust.edu.tw

Supported by the National Science Council under grant NSC- 101-2628-E-011-001.
Submitted to Journal of Neuroimaging.

J Neuroimaging 2014;00:1-7.
DOI: 10.1111/jon.12085

Introduction

Functional magnetic resonance imaging (fMRI) is used to estimate brain function and neuronal activities. The in vivo fMRI technique[1] introduced in 1992 is a critical scientific development. Since 1992, fMRI has become an essential tool in neuroscience research. Early fMRI research generally focused on task-based studies. Task-based studies require participants to perform a specific task (eg, tapping a finger or answering questions) according to a tailored time sequence or paradigm. Researchers then predict the signal response by using specific models, such as a hemodynamic response function, and use statistics to identify brain areas related to the performed task.

Research has suggested that intrinsic activity affects overall brain function.[2] This intrinsic activity may represent spontaneous cognition, which task-based fMRI is unlikely to measure. In 1995, Biswal measured function connectivity in the motor cortex of a resting human brain by using fMRI.[3] Resting-state fMRI (rsfMRI) is now used to investigate brain functional connectivity. rsfMRI studies have demonstrated that the spontaneous neuronal activity of human brains exhibits low-frequency fluctuations in signal time courses in magnetic resonance images. The coherence of low-frequency fluctuations is called functional connectivity (FC). Regions with high FC between each other constitute a resting-state network (RSN). rsfMRI can be used to investigate brain functional network structure and psychiatric disorders.[4] Compared with task-based fMRI, resting-state experiments are relatively relaxing because they require neither task design nor stimulated states. Subjects are requested to rest in the MRI scanner and not think of anything in particular. rsfMRI is used for neurological diseases including Alzheimer's disease,[5] autism,[6] and attention-deficit hyperactivity disorder.[7] Of all observed RSNs, the default mode network (DMN) is a highly reproducible network. Research has suggested that the DMN is associated with integrating cognitive functions, emotional processing, and daydreaming.[8]

The fMRI signal fluctuation of resting-state activities occurs mainly in a low-frequency range (approximately less than .15 Hz),[9,10] which is close to the frequency of human physiological motions such as respiration and cardiac pulsation. Physiological motions can induce signal modulations in fMRI time series.[11] Overlapping frequency ranges between physiological motion and resting-state activities reduce the reliability of rsfMRI. Generally, rsfMRI studies manage this issue by using regression analysis. Regression removes nuisance variances caused by factors such as physiological motion, head movements, and baseline drifts.

However, it is unclear whether regression analysis should be performed, especially for the nuisance variance estimated using a global mean.[12] For example, research has indicated that global mean regression affects FC results[9] and has suggested that using regression is a valid and useful processing method.[12] However, studies have supported that global signal regression does not yield a correction that reveals underlying neuronally induced fluctuations.[13,14] In addition, the existence of an anticorrelated network in global regression is controversial.[12–16]

This study explores the effects of regression analysis when using different combinations of nuisance variances on in vivo rsfMRI data sets. The purpose of this study was to identify an appropriate analysis procedure for future rsfMRI studies by comparing FC results obtained using different regression methods.

Materials and Methods

Participants and In Vivo Experiment

We performed all imaging experiments by using a 3.0 Tesla whole-body MRI system (Siemens, Skyra, Erlangen, Germany) equipped with a 32-channel head coil. Twenty volunteers (10 men and 10 women; aged 23.4 ± 1.5 years) participated in the experiments after providing institutionally approved consent. We first obtained scout localizers and selected 33 transversal slices of the whole brain. The rsfMRI protocol contains a gradient-echo echo-planar-imaging (EPI) sequence. The following EPI imaging parameters were applied: TR/TE of 2000/30 milliseconds, 220-mm FOV, 5-mm slice thickness, 4 dummy scans, 204 measurements, and a matrix size of 64×64. The total scan time was approximately 7 minutes. Anatomical images were acquired using a 3D MP-RAGE sequence to co-register all participants. The following imaging parameters for the 3D MP-RAGE were applied: TR/TE of 2530/1.64 milliseconds, 256-mm FOV, 7° flip angle, 176 sagittal slices, a matrix size of 256×256, a voxel size of 1×1×1 mm, and a nonselective inversion preparation with an inversion time of 1,100 milliseconds.

Image Preprocessing Procedure

Each participant's data were transferred offline to a personal computer and processed using Matlab® (Mathworks, Natick, MA, USA), a statistical parametric mapping (SPM) system, and data processing assistant for resting-state fMRI (DPARSF). SPM and DPARSF are available online (SPM:http://www.fil.ion.ucl.ac.uk/spm; DPARSF:http://www.restfmri.net). The first four dummy-scan volumes were discarded during the image preprocessing procedure. The remaining 200 measurements underwent slice timing to correct timing inconsistencies in each volume and image realignment to correct temporal image shifts caused by head movements. Subsequently, image volumes were normalized to Montreal Neurological Institute (MNI) coordinates and the voxel size was resampled to 3×3×3 mm. The matrix size of the obtained volume was 61×73×61. Each volume was smoothed using a Gaussian filter set to full width half maximum (FWHM) at 4×4×4 mm. Spatial smoothing suppressed noise and individual differences in gyral and sulcal anatomy. A temporal bandpass filter (.01-.08 Hz) was applied to the volumes to reduce physiological noise.

Regression of Nuisance Variances

Three types of nuisance variance are typically estimated in rsfMRI research: (1) six motion parameters obtained after a motion correction procedure; (2) time-intensity courses averaged across cerebrospinal fluid (CSF) voxels and white matter (WM) (referred to as the CSF curve and WM curve); and (3) a signal time course averaged across voxels for the entire brain (referred to as the global curve). The resting-state experiment generally lasts longer than 5 minutes, during which the participant could move his or her head. Motion parameters can be regressed to reduce motion-related noise. Research has suggested that regressions of the CSF curve, WM curve, and global curve can reduce physiological noise or baseline drift.[17]

We compared the FC results of the DMN by using different combinations of nuisance variances, including six motion parameters and the WM curve, CSF curve, and global curve. The regression analyses corresponding to these variances are expressed as motion-reg, WM-reg, CSF-reg, and global-reg, respectively. We obtained the six motion parameters after realigning EPI volumes. We produced the WM curve and CSF curve by using the built-in CSF and WM masks of DPARSF in the MNI152 space. We obtained the global curve by averaging the signal of all brain voxels in each EPI volume and conducted regressions of nuisance variances by using $R=(I-X(X^TX)^{-1}X^T)$ where y is a vector containing a time series of preprocessed EPI volumes, X is a matrix consisting of predictor signal variance, and R represents the regression analysis results. R was a time series with the nuisance variances removed.

This study investigated the effects of five combinations of four nuisance variances (motion, CSF curve, WM curve, global curve). Regressing the four nuisance variances was suggested in the literature.[18] The five following combinations were used: method 1 (M1): no regression; M2: motion-reg; M3: motion-reg; CSF-reg and WM-reg; M4: motion-reg and global-reg; and M5: motion-reg, CSF-reg, WM-reg, and global-reg.

Analysis of the Functional Connectivity of the DMN

We derived FC results after data preprocessing by using two methods, node analysis and FC mapping. Node analysis was performed to calculate Pearson's correlation coefficients (r) between signal time courses obtained from each DMN node,[19] including the posterior cingulate cortex (PCC), ventral medial prefrontal cortex (VMPFC), inferior parietal lobule (IPL), lateral temporal cortex (LTC), dorsal medial prefrontal cortex (DMPFC), and parahippocampal gyri. Table 1 shows the MNI coordinates of the 13 nodes. Node analysis produced a 13×13 FC matrix based on each data set (M1 to M5) from each participant.

For FC mapping, a seed-based correlation method was used to produce whole-brain FC maps in which the seed point was located in the PCC (MNI coordinate: −5, −49, 40). The FC-mapping procedure was conducted to create FC maps by using a voxel-by-voxel calculation of r-values between the signal time courses obtained from each voxel and those in the PCC. The time course of each node (or seed point) was obtained by

Table 1. The MNI Coordinates

	Coordinates(*x*, *y*, *z*)	Seed Region
Node 1	−4, 50, −11	Medial prefrontal cortex (ventral)
Node 2	−1, 55,−17	Medial prefrontal cortex (anterior)
Node 3	−5,−49, 40	Posterior cingulate cortex
Node 4	−43,−60, 30	Left lateral parietal cortex
Node 5	45, −60, 29	Right lateral parietal cortex
Node 6	−7, 44, 48	Left superior frontal cortex
Node 7	20, 46, 49	Right superior frontal cortex
Node 8	−57, −17, −16	Left inferior temporal cortex
Node 9	54, −6, −16	Right inferior temporal cortex
Node 10	−22,−32, −8	Left parahippocamal gyrus
Node 11	17, −26, −8	Right parahippocamal gyrus
Node 12	12, 52, 31	Cerebellar tonsils
Node 13	5,−52, 9	Retrosplenial

The MNI coordinates of the 13 nodes in the default mode network.

averaging the signal time course of the seven voxels surrounding the node. The sampling distribution of r was not normally distributed. Therefore, for subsequent data analysis, the r-values obtained in both analyses were transformed to Fisher's z-values by using Fisher's r-to-z transformation. Fisher's z-value is the inverse hyperbolic tangent of r, given by $Z = \tanh^{-1} r$ where z refers to Fisher's z. 3D FC maps were generated using the data sets (M1 to M5) from each participant and five mean 3D FC maps for all participants.

Statistical Analysis

We generated 100 FC matrices (20 participants, 5 data sets) to assess the FC differences between the different regression methods. We used a Student's t-test to analyze these differences and considered differences statistically significant when $P < .01$. We calculated the means, standard deviations (SDs), and coefficients of variations (COVs) of the FC matrices across all participants.

Results

Figure 1 displays the means, SDs, and COVs of the 13×13 FC matrices calculated using data sets M1 to M5. A paired Student's t-test revealed that the five mean FC matrices were significantly different from each other ($P < .01$). The FC matrices were separated into two groups based on appearance (Group 1: M1, M2, and M3; Group 2: M4 and M5). In Group 1 (G1), the mean FC values gradually decreased from M1 to M3. The mean FC for each node-to-node connection in Group 2 (G2) was significantly lower than those in G1. Most elements in the COV matrices of G2 were higher than those of G1. The main difference between G1 and G2 was global-reg. We performed paired t-tests on FC matrices obtained using different regression methods (M1 to M5). Figure 2 displays the P-value matrices of all comparisons. Figure 3 shows the FC values between the PCC and the other 12 nodes. It displays the FC means, SDs, and COVs obtained by conducting node analysis. The values were extracted from the third row of each FC matrix shown in Figure 1.

Figure 4 displays the average FC maps calculated using all data sets (M1 to M5). Figure 4a shows color-coded FC maps. Figure 4b shows FC maps in which the Fisher's z thresholds ($z > .2$ or $z < .2$) are superimposed onto T1-weighted images. The anticorrelated areas, indicated in purple in M3 to M5, were absent in M1 and M2. Anticorrelated voxels from the M3 data set were mainly distributed inside brain ventricles. This is most likely false connectivity. The observation of anticorrelated areas in M4 and M5 is consistent with previously reported results.[12,18,20] In M4 and M5, the FC values in the left and right parahippocampal gyri are mostly less than .2, and, thus, are not seen in Fig. 4b.

Discussion and Conclusion

This study investigated whether regression analysis is required in rsfMRI preprocessing and whether anticorrelations observed in rsfMRI are artificially introduced by global-curve regressions. We compared the FC results obtained when using five combinations of regression methods (M1 to M5) and two data analysis schemes (node analysis and FC mapping).

Node analysis demonstrated the FC between each of the 13 nodes. The mean Fisher's z-values were lower in G2 than in G1. COVs were prominently higher in G2 than in G1. The FC matrices, showing correlations between time courses of the 13 DMN nodes, demonstrated the same mean, SD, and COV trends. The major difference between G1 and G2 was the introduction of global-reg. Therefore, the results of node analysis indicate that global-reg increases inter-subject FC variation. The result of node analysis seems suggesting that global-reg degrades rsfMRI analysis. Although this result is consistent with the findings of Murphy et al.,[13] Chang et al.[21] suggested that unmodeled noises, such as nonlinear interactions between physiological effects, may contribute to the global signal. Global regression may thus be useful for identifying anticorrelated regions in correlation analysis.

Although Fisher's z-values of the whole brain decreased dramatically after applying global-reg, we were still able to identify most DMN nodes based on Fisher's z-values based on the 3D FC volumes by using the z threshold of .2. Global-reg generated brain areas anticorrelated with the PCC. The anticorrelated areas were not observed in G1, which did not undergo global-reg. The anticorrelated brain areas were the same areas identified in previous studies.[9,12] The DMN is generally called the task-negative network (TNN) because it deactivates when a participant performs a range of tasks. By contrast, the network anticorrelated to the DMN is called the task-positive network (TPN). Abnormal TPNs have been linked to variability in patient groups. Therefore, FC mapping results support using global-reg for rsfMRI analysis, especially when the focus is anticorrelated networks.

Applying the two analysis methods to the same data sets leads to two opposing conclusions regarding global-reg. Global-reg significantly reduces Fisher's z-values and increases inter-subject COVs. When using global-reg, the FC of several nodes is lower than the preset threshold (.2). However, global-reg generates anticorrelated networks that are relevant, according to several MRI studies[12,15,20,22] and an electrophysiological study.[23]

The purpose of this study was to optimize the analysis procedure and provide a direction for future data-processing

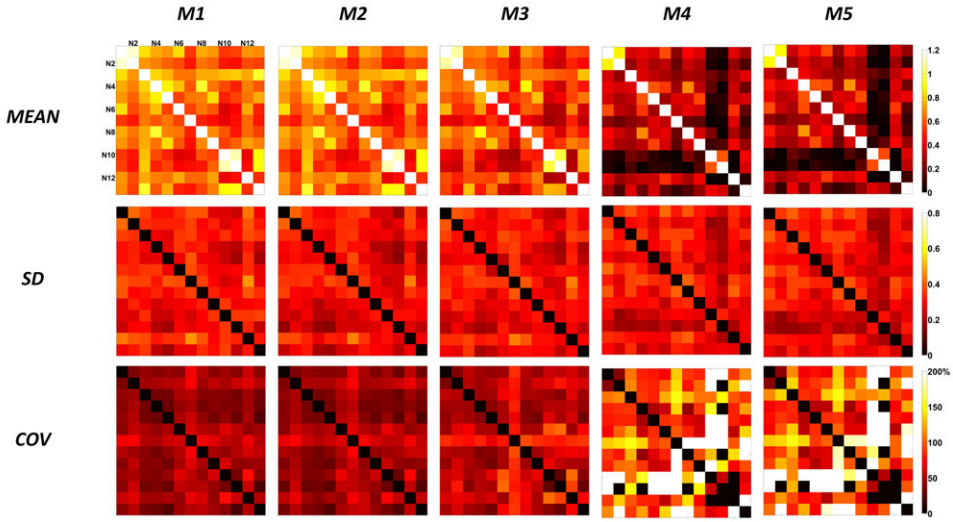

Fig 1. FC Fisher's *z* matrices (mean, SD, and COV) obtained using the five regression methods. N 2 to N 12 represent nodes 2 to 12.

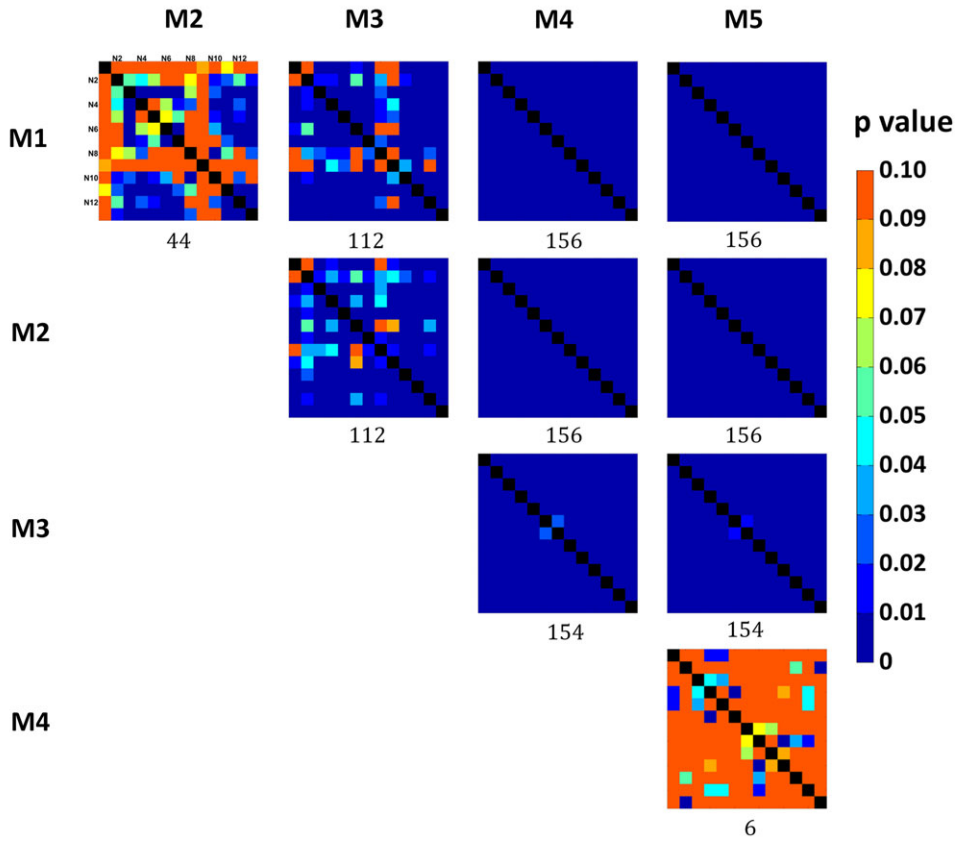

Fig 2. The results of *t*-tests performed between FC matrices obtained using different combinations of regression methods (*P*-values of paired *t*-test, n = 20). The numbers of FC matrix elements with significant differences are noted beneath each image.

procedures for rsfMRI. According to the results, M3 is not suggested because we identified false connectivity in WM in the data sets processed using M3. This study does not show significant improvement when applying motion-reg. However, previous studies, such as the study of Lund et al.,[24] have shown the effectiveness of motion-reg in fMRI analysis. If motion correction is desired and M3 is discarded, the remaining methods are M2, M4, M5. According to node analysis (Fig 2), the differences in the results obtained using M4 and M5 are mostly nonsignificant. Because M5 has been widely used in previous studies,[18,19]

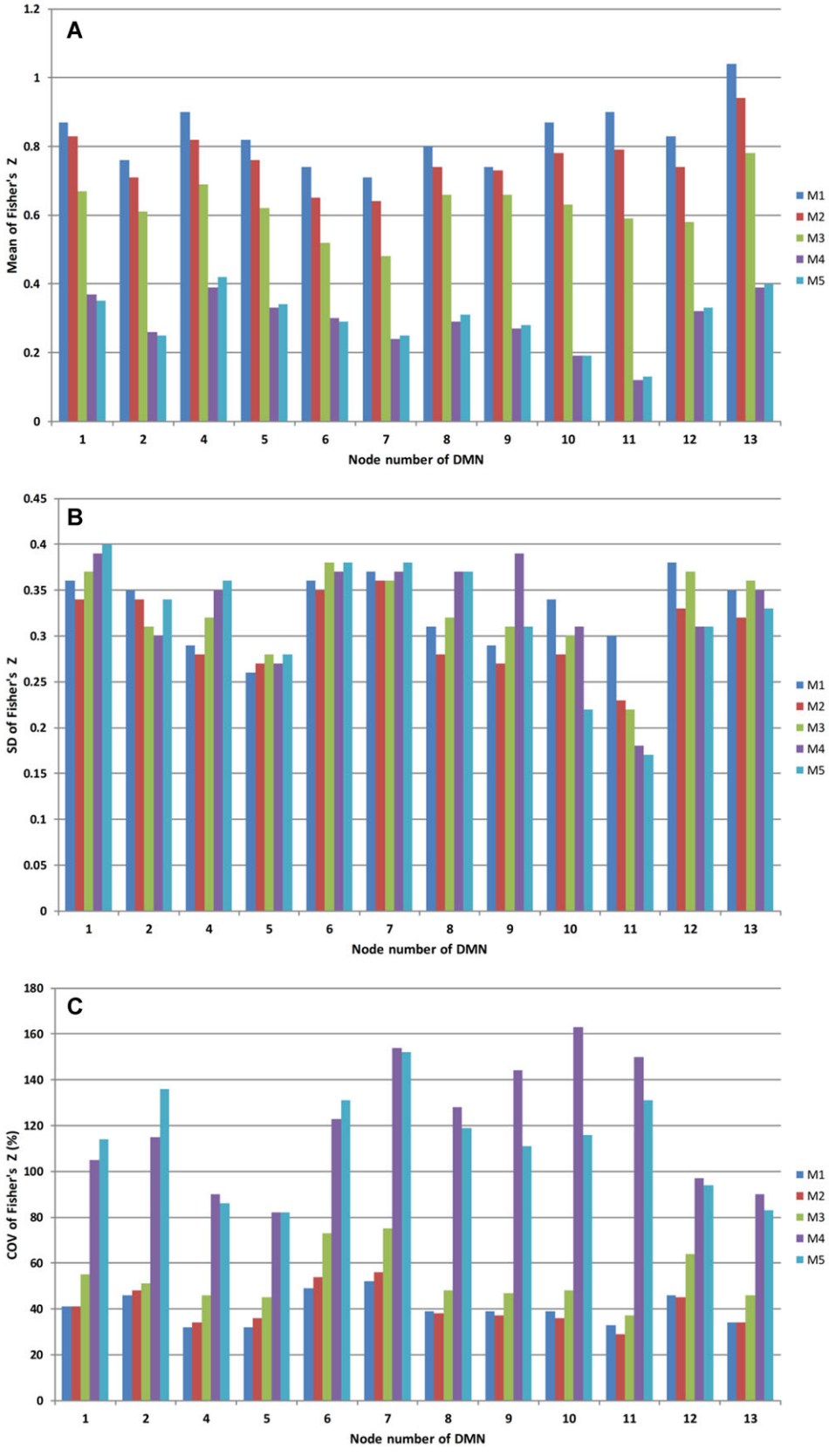

Fig 3. The mean (a), SD (b), and COV (c) for Fisher's *z*-values obtained between the PCC and 12 DMN nodes using the five regression methods.

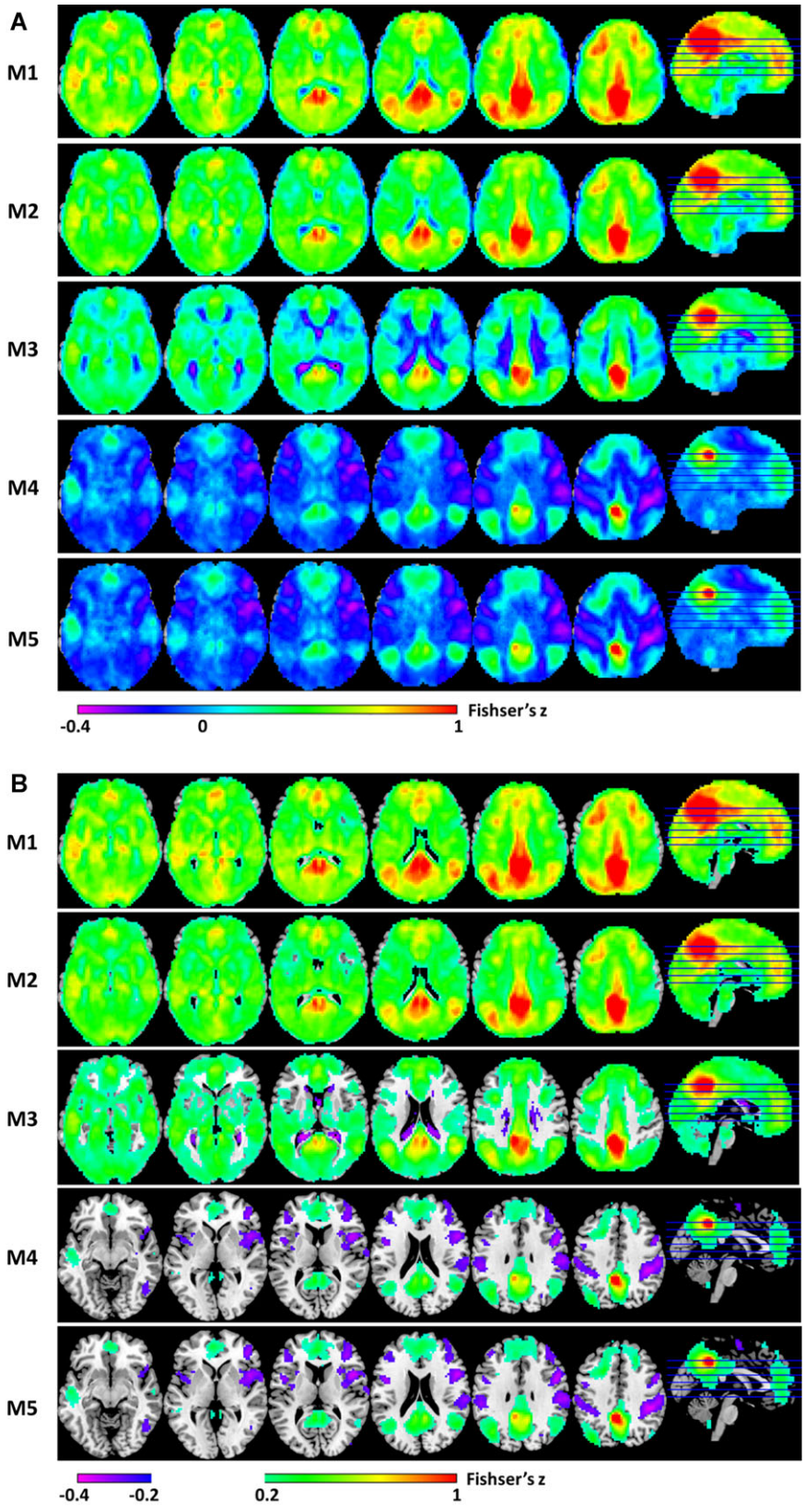

Fig 4. FC maps of the DMN obtained using different regression methods. (a) Fisher's *z* maps without thresholds; (b) Fisher's *z* maps with thresholds ($z > .2$ or $z < .2$).

M5 is more favorable than M4 to compare the rsfMRI results with those of previous studies. The overall comparison supported applying both M2 and M5 to generate two data sets and performing group statistics by using both data sets. rsfMRI data must be interpreted carefully if the data sets processed using the two regression methods lead to different conclusions.

In this study, we chose correlation analysis as our research target. In the rsfMRI literature, both independent-component analysis (ICA) and correlation analysis have been widely used. ICA, which separates signals into independent components, is used to identify rsfMRI networks and to remove high- and low-frequency noise. The ability to remove noise renders comparison of the regression method complex. For example, the global signal may be extracted as an independent component in ICA analysis, producing an effect similar to global signal regression. The impact of signal regression on ICA analysis warrants future research. In this study, we did not record physiological signals such as cardiac pulsation and respiratory motion. Therefore, we did not perform data regression using physiological signals. This is a limitation of the present study. Cardiac pulsation and respiration motion are both influential factors in rsfMRI analysis. For example, Chang et al.[21] showed that physiological correction increased the extent of negative correlations and reduced the extent of positive correlations. In addition, they also demonstrated that anticorrelated networks could be observed when using physiological noise correction. The effect of physiological repressors combined with the four widely used regressors (motion-reg, WM-reg, CSF-reg, global-reg) merits future research. In conclusion, data regression plays a major role in rsfMRI studies. Data sets processed using regression methods should be interpreted carefully.

References

1. Kwong KK, Belliveau JW, Chesler DA, et al. Dynamic magnetic resonance imaging of human brain activity during primary sensory stimulation. *Proc Natl Acad Sci USA* 1992;89:5675-5679.
2. Buzsaki G, Kaila K, Raichle M. Inhibition and brain work. *Neuron* 2007;56:771-783.
3. Biswal B, Yetkin FZ, Haughton VM, et al. Functional connectivity in the motor cortex of resting human brain using echo-planar MRI. *Magn Reson Med* 1995;34:537-541.
4. Greicius M. Resting-state functional connectivity in neuropsychiatric disorders. *Curr Opin Neurol* 2008;21:424-430.
5. Greicius MD, Srivastava G, Reiss AL, et al. Default-mode network activity distinguishes Alzheimer's disease from healthy aging: evidence from functional MRI. *Proc Natl Acad Sci USA* 2004;101:4637-4642.
6. Kennedy DP, Courchesne E. The intrinsic functional organization of the brain is altered in autism. *Neuroimage* 2008;39:1877-1885.
7. Zang YF, He Y, Zhu CZ, et al. Altered baseline brain activity in children with ADHD revealed by resting-state functional MRI. *Brain Dev* 2007;29:83-91.
8. Buckner RL, Andrews-Hanna JR, Schacter DL. The brain's default network: anatomy, function, and relevance to disease. *Ann N Y Acad Sci* 2008;1124:1-38.
9. Greicius MD, Krasnow B, Reiss AL, et al. Functional connectivity in the resting brain: a network analysis of the default mode hypothesis. *Proc Natl Acad Sci USA* 2003;100:253-258.
10. Lowe MJ, Mock BJ, Sorenson JA. Functional connectivity in single and multislice echoplanar imaging using resting-state fluctuations. *Neuroimage* 1998;7:119-132.
11. Glover GH, Li TQ, Ress D. Image-based method for retrospective correction of physiological motion effects in fMRI: RETROICOR. *Magn Reson Med* 2000;44:162-167.
12. Fox MD, Zhang D, Snyder AZ, et al. The global signal and observed anticorrelated resting state brain networks. *J Neurophysiol* 2009;101:3270-3283.
13. Murphy K, Birn RM, Handwerker DA, et al. The impact of global signal regression on resting state correlations: are anti-correlated networks introduced? *Neuroimage* 2009;44:893-905.
14. Saad ZS, Gotts SJ, Murphy K, et al. Trouble at rest: how correlation patterns and group differences become distorted after global signal regression. *Brain Connectivity* 2012;2:25-32.
15. Chai XJ, Castanon AN, Ongur D, et al. Anticorrelations in resting state networks without global signal regression. *NeuroImage* 2012;59:1420-1428.
16. Wong CW, Olafsson V, Tal O, et al. Anti-correlated networks, global signal regression, and the effects of caffeine in resting-state functional MRI. *Neuroimage* 2012;63:356-364.
17. Shmueli K, van Gelderen P, de Zwart JA, et al. Low-frequency fluctuations in the cardiac rate as a source of variance in the resting-state fMRI BOLD signal. *Neuroimage* 2007;38:306-320.
18. Fox MD, Snyder AZ, Vincent JL, et al. The human brain is intrinsically organized into dynamic, anticorrelated functional networks. *Proc Natl Acad Sci USA* 2005;102:9673-9678.
19. Fair DA, Cohen AL, Dosenbach NU, et al. The maturing architecture of the brain's default network. *Proc Natl Acad Sci USA* 2008;105:4028-4032.
20. Wong CW, Olafsson V, Tal O, et al. Anti-correlated networks, global signal regression, and the effects of caffeine in resting-state functional MRI. *NeuroImage* 2012; 63(1):356-364.
21. Chang C, Glover GH. Effects of model-based physiological noise correction on default mode network anti-correlations and correlations. *Neuroimage* 2009;47:1448-1459.
22. Carbonell F, Bellec P, Shmuel A. Global and system-specific resting-state fMRI fluctuations are uncorrelated: principal component analysis reveals anti-correlated networks. *Brain Connectivity* 2011;1:496-510.
23. Popa D, Popescu AT, Pare D. Contrasting activity profile of two distributed cortical networks as a function of attentional demands. *J Neurosci* 2009;29:1191-1201.
24. Lund TE, Norgaard MD, Rostrup E, et al. Motion or activity: their role in intra- and inter-subject variation in fMRI. *Neuroimage* 2005;26:960-964.